Synthesis, complexation properties and spectroscopic studies of the cation-induced conformational changes of some new oligooxaethylene-spacered diporphyrin arrays†

Laura La Monica,[a] Donato Monti,*[a] Giovanna Mancini,[b] Marco Montalti,[c] Luca Prodi,*[c] Nelsi Zaccheroni,[c] Giuseppe D'Arcangelo[a] and Roberto Paolesse[a]

[a] *Dipartimento di Scienze e Tecnologie Chimiche, Universita' degli Studi di Roma "Tor Vergata", I-00133 Rome, Italy*
[b] *Centro C.N.R. di Studio sui Meccanismi di Reazione, Dipartimento di Chimica, Universita' degli Studi di Roma "La Sapienza", I-00185 Rome, Italy*
[c] *Dipartimento di Chimica "G. Ciamician", Università di Bologna, I-40126 Bologna, Italy*

Received (in Cambridge, UK) 3rd October 2000, Accepted 16th January 2001
First published as an Advance Article on the web 16th March 2001

New linear diporphyrin arrays and a heteroleptic diad have been synthesized in good yield. ^{1}H NMR, UV-visible and fluorescence studies reveal that the receptors bind to alkali and alkaline-earth metal ions to give a supramolecular complex in which the ion is nestled within the oligooxaethylene framework. The formation of the host–guest complexes promotes a change in the geometry of the system toward a topology in which the two tetrapyrrolic macrocycles tend to face together. This is evidenced by the mutual ring current anisotropy effect exerted by the porphyrinic platforms, and by the blue shift and broadening of the relative UV-visible bands (Soret). In particular, the changes observed allow the complexation process to be monitored at very low concentrations. The association constants lie within the range 25–1 $\times$ 10^5 M^{-1} (CD_3CN–$CDCl_3$ 1 : 1) depending on either the nature of the diporphyrinic receptors or that of the interacting metal ions. The heteroleptic diad shows a very efficient energy transfer process (>99%) between the two different macrocycles in a variety of solvents that is not altered by complexation with metal ions. The systems reported present interesting properties as switchable biomimetics.

Introduction

The rich chemistry of porphyrin dimers and oligomers constitutes a challenging and stimulating arena of research devoted to the construction of biomimetic models[1] of the light harvesting antenna apparatus of bacteria and green plants.[2] Moreover, cofacial[3a,b] and the closely related, more flexible, "Pac-Man"[3c,d] metallodiporphyrins are regarded as excellent tools for multielectron redox activation of small molecules, mimicking the activity of metalloenzymes involved in life-sustaining cycles such as peroxidases, cytochrome P-450, cytochrome c oxidase and nitrogenase.[4]

We recently reported[5] on the synthesis and preliminary binding properties of a linear tetraoxaethylene-spacered diporphyrin array, able to undergo a conformational change toward a cofacial topology upon interaction with alkali metal ions. This strategy, in which some critical covalent bonds are replaced by non-covalent interactions, would represent a promising alternative to either the non-covalent or the fully covalent[6] approaches usually pursued for the construction of diporphyrin systems with cofacial topology. Moreover, the possibility of tuning the geometry makes the systems investigated particularly appealing and prone to applications, for example in the field of molecular switches or sensors.[7]

Prompted by the promising results obtained, we extended the studies to a wider class of diporphyrin receptors, namely **1a**–**1c** and **2** (Chart 1). The unsymmetrical diad **2** could allow the achievement of a system in which the different substitution pattern would result in interesting photophysical properties.[1c] A systematic study of the interaction of such derivatives with a series of alkali and alkaline-earth metal ions has been undertaken in order to acquire information on the effect of the structural features of the partners involved on the conformational changes of the diporphyrin systems investigated. The strength of the ion–receptor interaction has been evaluated by means of ^{1}H NMR spectroscopy, which additionally gave some indication of the actual change of geometry of the systems. A nice parallelism has been evidenced by concomitant UV-visible or fluorescence spectroscopy.

Results and discussion

Synthesis

The systems studied are characterised by a different number of oxygen donor sites (*e.g.* length of the oligooxaethylene spacer) as well as by the presence of two additional methoxy functionalities on the aromatic part of the linkers, with respect to the previously reported system.[5] This should confer better coordination properties toward the investigated metal ions. The diporphyrin arrays **1a**–**1c** were prepared in a straightforward way by following a modified procedure reported earlier,[5,8] which is outlined in Scheme 1(a). Condensation of pyrrole and 4-hydroxy-3-methoxybenzaldehyde (vanillin), in the presence of a tenfold excess of benzaldehyde in refluxing acetic acid, afforded, besides the expected *meso*-tetraphenylporphyrin

† Electronic supplementary information (ESI) available: ^{1}H NMR titration curves for receptor **1c** and titration spectra of **1b**. See http://www.rsc.org/suppdata/nj/b0/b008250n/

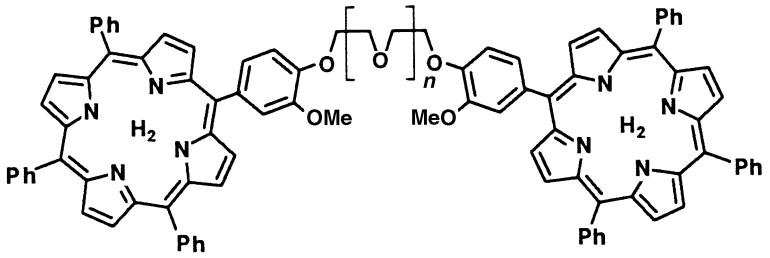

1a, b, c: $n = 2, 3, 4$

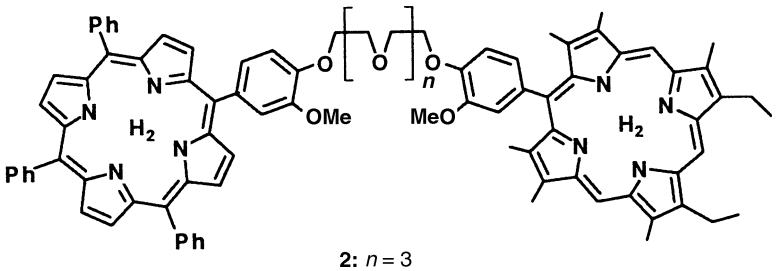

2: $n = 3$

(H_2TPP), the desired 5-(4-hydroxy-3-methoxyphenyl)-10,15, 20-triphenylporphyrin **3a** in satisfactory yield, after standard work-up and chromatographic separation. The use of an excess of benzaldehyde was necessary in order to drive the cyclisation toward selective formation of the monoaryl-substituted porphyrinic derivative. The porphyrin derivative **3a** was coupled with tri-, tetra- and penta-ethylene glycol ditosylate under Williamson conditions[9] to give in good yield the targets **1a**–**1c**, respectively. The procedure for the synthesis of the unsymmetric diporphyrin **2** is slightly different (Scheme 1b) from that above. Attempts to prepare **2** by direct coupling of the oligoethylene glycol ditosylate in the presence of equi-

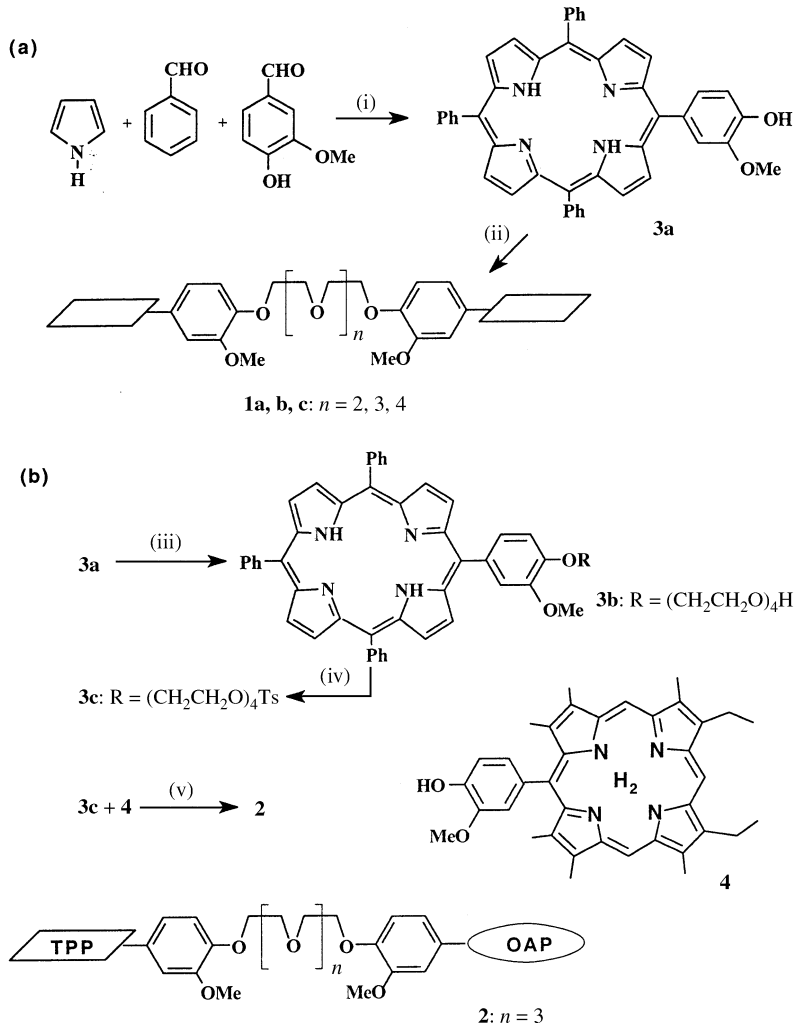

Scheme 1 (a) Synthesis of diporphyrin derivatives **1a**–**1c**. Reagents and conditions: (i) acetic acid, reflux, 3 h, yield 12%; (ii) tri-, tetra-, or penta-ethylene glycol ditosylate, anhydrous K_2CO_3, DMF, 80 °C, 12 h, 80%. (b) Synthesis of diporphyrin derivative **2**. (iii) $HO(CH_2CH_2O)_3$-CH_2CH_2OTs, anhydrous K_2CO_3, DMF, 80 °C, 12 h, 90%; (iv) TsCl, dry pyridine, r.t., 12 h, 80%; (v) **4**, anhydrous K_2CO_3, DMF, 80 °C, 12 h, 20%. Ts = *p*-Toluenesulfonyl.

molar amounts of both the aryl- and alkyl-porphyrin precursors resulted in a mixture of hetero- and homo-diporphyrin derivatives requiring tedious chromatographic separation. Alternatively, the arylporphyrin precursor (**3a**) was coupled with tetraethylene glycol monotosylate to give the corresponding ω-monoporphyrinyl derivative **3b**. This was converted into the corresponding tosyl derivative (*p*-toluenesulfonyl chloride, CH_2Cl_2, pyridine) **3c**, which was in turn coupled with the octaalkylporphyrin (OAP) moiety **4** to give the desired heterodiad **2** in 15% overall yield. The alkylporphyrin **4** was straightforwardly obtained by acid-catalysed cyclisation of the relative biladiene-*a,c* precursor[10] with vanillin.

The above porphyrin derivatives have been characterised by UV-visible, ^1H, ^{13}C NMR and FAB-MS techniques. The proton NMR spectra ($CDCl_3$) show features of both the oligooxaethylenic spacers and of the porphyrinic platforms, within the examined concentration window (up to 5×10^{-4} M). Details are reported in the Experimental section. FAB-MS spectra provide further evidence for formation of the desired architectures; showing molecular clusters at the expected *m/z* values.

Spectroscopic studies

The UV-visible spectra (1×10^{-6} M $CHCl_3$–CH_3CN 1 : 1, v/v) of the diporphyrin architectures are virtually superimposable on the algebraic sum of those of their parent monomers, indicating that the electronic interaction between the two macrocycles in the dimers is in all cases relatively weak. The spectra feature the typical Soret band (402–419 nm), and the four visible Q bands in the range 515–650 nm. The fluorescence quantum yields and the excited states lifetimes are typical of the parent monomers. In these systems the only additional pathway responsible for a radiationless decay to the ground state, due to the formation of dimeric structures, is an electron-transfer process between the two porphyrin units, which for such systems is thermodynamically forbidden.[1e,11] In the case of the unsymmetric diad **2**, characterised by the presence of both a TPP (triphenylporphyrin) and an OAP (octaalkylporphyrin) unit, the typical fluorescence band of the latter macrocycle could not be observed, even when the excitation light was prevalently absorbed by this moiety. On the contrary, the typical band of the TPP component is present, with an excited state lifetime equal to that of the monomeric species. The excitation spectra were very indicative for understanding the behaviour of this compound. Positioning the monochromator emission at $\lambda_{em} = 725$ nm, where the fluorescence is almost entirely (>95%) due to the TPP component, the excitation spectrum is almost the same as the absorption spectrum of the whole compound, showing bands of both the TPP and OAP components, with their relative intensity unchanged. All these findings clearly indicate the occurrence of a thermodynamically allowed efficient energy-transfer mechanism from the OAP to the TPP moiety. A limiting value for the rate constant of the energy transfer process (k_e) of 1×10^{10} s^{-1} can be calculated, on the basis of a residual fluorescence intensity of the OAP moiety lower than 1% of that observed for the unquenched chromophore. This leads to the assumption that the whole process occurs with an efficiency higher than 99%. An electron transfer process was reported to be, in similar cases, slightly endoergonic[1e] and for this reason it can not compete with a very fast energy transfer process.

It is important at this point to compare the experimental rate constants with theoretical ones for the energy-transfer process. In particular, an energy-transfer process can be described in terms of a Coulombic (Föster)[12a] and an exchange (Dexter)[12b] mechanism. For similar diporphyrin systems, the Föster mechanism was preferred for explaining the experimental results.[1e,13] To estimate the energy-transfer rate constant, according to this mechanism, the overlap integral between the emission spectrum of the donor $F(\nu)$ (normalised such that $\int F(\nu)d\nu = 1$) and the absorption spectrum of the acceptor $\varepsilon(\nu)$, J_F, has to be calculated (eqn. 1), resulting, for this dimer, in 1.75×10^{-14} cm^6 $mmol^{-1}$. The energy-transfer rate constant is finally expressed by eqn. 2 where n is the refractive index of the solvent, Φ and τ are the luminescence quantum yield and lifetime of the donor, J_F is the overlap integral and K^2 a geometric factor, which depends on the relative orientation of the dipoles and that, in our case, can be taken with confidence as 2/3.[12a] With a rate limiting constant of 1×10^{10} s^{-1}, it is possible to estimate, from eqn. 2, the distance between the two chromophores in solution, which is lower than 12.5 Å.

$$J_F = \int F(\nu)\varepsilon(\nu)\nu^{-4}\,d\nu \Big/ \int F(\nu)\,d\nu \quad (1)$$

$$k_e = \frac{8.8 \times 10^{-25} K^2 \Phi}{n^4 \tau r^6} J_F \quad (2)$$

Notably, the efficiency of the energy transfer did not change on changing the solvent polarity, *i.e.* from cyclohexane to pure acetonitrile, in contrast to what was reported[14] for a system having a similar poly(oxaethylene) bridge, and polypyridine complexes of Ru and Os as energy donor and acceptor, respectively. In our case the efficiency was >99% in all the solvents examined, so that the photoinduced energy-transfer process in **2** could not be used to probe solvent-dependent conformational changes of the bridge.

Interaction with metal ions

^1H NMR spectroscopy is a convenient technique for studying the binding of the above systems with metal ions. The experiments have been carried out in CD_3CN–$CDCl_3$ (1 : 1 v/v) in order to achieve the optimal solubility of the species investigated. The salts employed were perchlorates or iodides. The typical downfield shift of the protons of the oxaethylene spacers[15] indicates the occurrence of binding at the ether sites. The mass spectra (FAB) of the diporphyrin receptors in the presence of an excess of metal salts (M^{n+}) gave further evidence for formation of the complexes. Peaks at [**1a**–**1c** + $M]^{n+}$, corresponding to the supramolecular adducts, are clearly visible in the spectral pattern of all the receptors investigated.[16]

Typical chemical shift changes of the signals of the porphyrin macrocycles clearly evidence conformational change of the receptors, promoted by interaction with the metal ions. A significant example is shown in Fig. 1, which shows the chemical shift changes of the porphyrin **1b** protons with increasing concentration of potassium salt. The evident upfield shift of the porphyrinic β-proton resonances, up to 200 Hz, is an indication of the change of topology toward cofacial geometry.

Negligible variations were observed in the case of the reference porphyrin **3a**. Moreover, neither the UV-visible nor the ^1H NMR spectral patterns of the diporphyrins studied show any appreciable variation upon addition of an excess (up to 5×10^{-2} M) of Bu_4NClO_4, ruling out the occurrence of selfaggregation phenomena induced by the increased ionic strength of the medium. It is possible to evaluate the strength of the metal–receptor interaction by a non-linear least-squares fitting analysis of the chemical shift variation of the selected signals *vs.* the concentration of the added metal ions (see ESI Fig. S1).† All the receptors investigated form a 1 : 1 complex with the metal cation as clearly evidenced by the excellent adherence of the experimental data to the calculated theoretical curve. The results obtained are shown in Table 1. As far as alkali-metal ions are concerned, the association constants vary within the range 25–6500 M^{-1}, depending on the nature of the cation and increasing with the number of oxygen coordi-

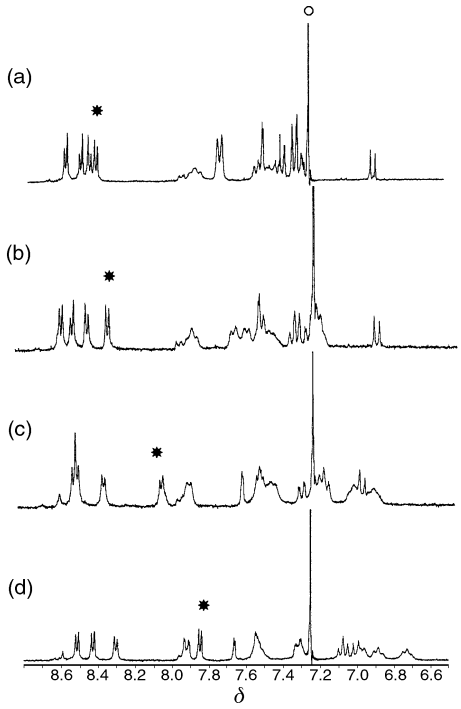

Fig. 1 ^{1}H NMR spectral variation (300 MHz, CD_3CN–$CDCl_3$ 1 : 1, v/v) of the selected aromatic part (*) of compound **1b** (3.5×10^{-4} M) in the presence of $KClO_4$: (a) 0, (b) 5.38×10^{-3}, (c) 9.68×10^{-3}, (d) 20.7×10^{-3} M. (○) indicates residual solvent.

nation sites of the receptor. Not surprisingly, the presence of an additional methoxy group on the aromatic end of the spacer results in an appreciable enhancement of the affinity for the considered metal ions by one order of magnitude.[17] The selectivity toward the inclusion of different metal ions depends on the nature of the receptors. Receptors **1b** and **1c** show the largest affinity for potassium, whereas the smaller **1a** preferentially binds Na^+. This finding is evidently the consequence of a fine balancing of enthalpic and entropic contributions, the *wrapping* of a longer ether chain around a smaller cation being disfavoured by the loss of conformational entropy.

The extent of the chemical shift variations, induced by metal ion complexation, is dependent on the nature of the partners involved and may give an indication of the geometry achieved by the systems.[18] Some selected data are given in Table 1. They are not straightforwardly rationalisable; nevertheless, some key points may be identified. It is important to point out that the limiting values do not strictly depend on the strength of the interaction, but rather on the size of the interacting metal ion and on the length of the spacer. As far as the peripheral porphyrinic β-protons are concerned, the highest shielding is, in most cases, promoted by the sodium cation which reaches its maximum effect in the interaction with the tetra-spacered ($n = 3$) **1b**. A different trend is found for the smaller Li^+, which features highest chemical shift variations in the case of the shorter tri-segmented receptor **1a**. The vanishingly small chemical shift variations observed in the case of the **1a**–Cs^+ interaction can be ascribed to the poor ability of the receptor to encircle the large cation, which, evidently, results in a wider distance between the two porphyrinic platforms.

The unsymmetrical diad **2** features a somewhat increased binding strength toward K^+, with respect to its **1b** counterpart (Table 1). This is also accompanied by an increased shielding effect on the corresponding proton resonances. This is, in the first instance, a consequence of a relief of steric hindrance mutually exerted by the porphyrin platforms upon cofacialisation. This interpretation is, however, in contrast to the results obtained from both the UV-visible and fluorescence studies (see below) which indicate a substantially lower degree of electronic interaction between the two macrocycles. An alternative explanation considers the increased electron density of the OAP moiety,[19] which can account for the more favourable cation–receptor electrostatic interaction, as well as for the observed increased ring current anisotropy effect.

The binding constants for the interaction of several alkaline-earth metal ions with the diporphyrin receptor **1b** span three orders of magnitude, within the range 4×10^2–1×10^5 M^{-1}, with a marked selectivity for the strontium cation. The strength of the interaction is higher, by one order of magnitude or more, with than that of monocationic counterparts of similar ionic radius[20] (Fig. 2) as a consequence of the increased electrostatic interaction. The increased affinity toward alkaline-earth metal ions is commonly encountered in the case of crown ethers and other macrocycles,[21] as well as for related complex acyclics.[22] In the latter cases, however, the selectivity toward Sr^{2+}, which is found in the case of **1b**, van-

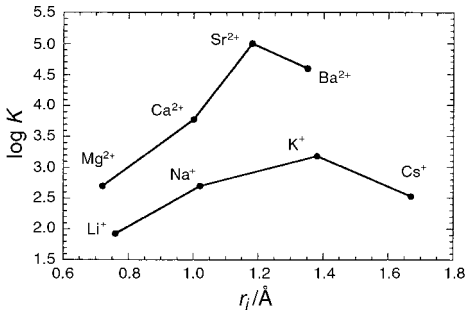

Fig. 2 Log K values (calculated from ^{1}H chemical shift changes, see text) for the interaction of alkali and alkaline-earth metal ions with receptor **1b** (CD_3CN–$CDCl_3$ 1 : 1, v/v) as a function of the ionic radii.

Table 1 Binding constant values (K/M^{-1})[a] for the interaction of diporphyrin receptors **1a**–**1c** and **2**, with alkali and alkaline-earth metal ions

	Receptor[c]			
Cation (r_i/Å)[b]	**1a**	**1b**	**1c**	**2**
Li^+(0.76)	85(−120)	70(−65)	160(−80)	
Na^+(1.02)	500(−140)	460(−20)	890(−80)	
K^+(1.38)	280(−20)	1500(−130)	6500(−45)	1850(−150)
Cs^+(1.67)	<25[d]	340(−50)	600(−80)	
Mg^{2+}(0.72)		490(−5)		
Ca^{2+}(1.00)		6100(−190)		
Sr^{2+}(1.18)		$>1 \times 10^5$(−100)		
Ba^{2+}(1.35)		$>4 \times 10^4$(−80)		

[a] In CD_3CN–$CDCl_3$ 1 : 1, v/v, at 25 °C. [b] Data taken from ref. 20. [c] Limiting complexation-induced chemical shifts ($\Delta\delta$/Hz, at 300 MHz) for the peripheral β-H protons are reported in parentheses. Negative values indicate upfield shifts. [d] Not determined. Variations below the instrumental detection limits.

ishes in favour of other alkali earth metal ions such as calcium or barium.

UV-visible and fluorescence studies of metal ion complexation

UV-visible and fluorescence studies give further insights on the cation-induced conformational changes of the diporphyrin systems. As far as the absorption spectra are concerned, addition of alkali and alkaline earth metal ions to $CHCl_3$–CH_3CN (1 : 1, v/v) solutions of the diads causes an appreciable change in intensity of the Soret band (380–440 nm, Table 2 and Fig. 3). This is accompanied by a small but significant blue shift of the absorption maxima, and an evident broadening, which indicate cofacial arrangement of the porphyrin–metal complexes.[3a] As also observed by ^1H NMR, the changes in the UV-visible spectra strongly depend on the length of the bridging unit, on the charge and size of the metal ion and on the nature of the porphyrin systems. In the case of the tri-segmented **1a**, for example, smaller changes were usually observed as a consequence of the steric strain suffered on approaching a pseudo-cyclic conformation. Diads featuring longer bridging units, and hence a greater conformational mobility, experience larger perturbations. In particular, for the tetra-spacered **1b**, Sr^{2+} and, to a somewhat smaller extent, Ba^{2+} form complexes for which the Soret band features the lowest intensity and the largest broadening (Fig. 3). It is of note that these changes are also accompanied by a new band at about 410 nm. This is usually accounted for as the consequence of an electronic interaction between porphyrin macrocycles held in a face-to-face type conformation.[3a,23] Conversely, in the case of the longer penta-spacered **1c**, the larger Ba^{2+} induces the strongest perturbation.

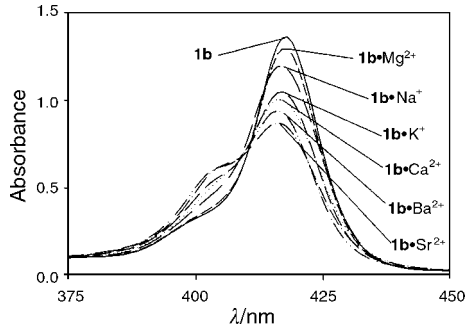

Fig. 3 UV-visible spectroscopic variation (Soret band) of diporphyrin receptor **1b** (1×10^{-6} M, CD_3CN–$CDCl_3$ 1 : 1, v/v) in the presence of an excess of added metal ions.

Table 2 UV-visible spectral data (λ_{max})[a] of diporphyrin receptors **1a**–**1c** and **2**, and their metal complexes[b]

Cation	1a	1b	1c	2
None	418(1.00)	418(1.00)	418(1.00)	417(1.00)
Na^+	417(0.82)	417(0.88)	417(0.82)	418(0.85)
K^+	417(0.93)	417(0.77)	417(0.83)	418(0.76)
Mg^{2+}	418(0.95)	418(0.95)	417(0.87)	417(1.00)
Ca^{2+}	416(0.97)	417(0.74)	416(0.95)	417(0.93)
Sr^{2+}	416(0.95)	416(0.64)	416(0.81)	419(0.79)
Ba^{2+}	418(0.93)	416(0.69)	416(0.77)	418(0.78)

[a] The relative absorbances (A_{rel}) are given in parentheses. [b] Porphyrin concentration: 1×10^{-6} M, (MeCN–$CHCl_3$ 1 : 1, v/v), 298 K.

In contrast to the absorption spectra, the fluorescence properties, in terms of the energy of the transition, quantum yield and excited state lifetime, are only slightly altered by the complexation with alkali and alkaline earth metal ions (Table 3). This is not, however, a completely unexpected result, since the transition responsible for the fluorescence process ($S_1 \rightarrow S_0$) is exactly the opposite ($S_0 \rightarrow S_1$) of that responsible for the Q bands in the absorption spectrum, that are also slightly perturbed upon complexation. It is interesting that the fluorescence of the unsymmetrical diad **2** is also perturbed by complexation only to a marginal extent. In this case the conformational changes caused by complexation, reducing the distance between the donor and acceptor moieties, are expected to increase the rate of the energy transfer process (eqn. 2). The efficiency of the process, however, can only slightly be increased, since it has been estimated to be greater than 99% even in the "free" ligand; as a consequence, also the fluorescence spectrum does not undergo any change upon addition of metal cations. These results do not exclude however the possibility of using these systems as prototypes for fluorescent chemosensors.[25] Although the fluorescence quantum yield is only slightly altered by complexation, it is still possible to monitor the presence of metal ions by means of photoluminescence spectroscopy. The observed fluorescence intensity is in fact proportional, when working in dilute conditions, both to the fluorescence quantum yield and to the molar absorption coefficient at the excitation wavelength. As a consequence, if excitation is performed in the Soret band, whose intensity decreases upon complexation, a decrease of the fluorescence intensity is also observed. By virtue of the reasonably high

A comparison between diporphyrin **1b** and its "hetero-homologue" **2**, characterised by the same tetraoxaethylene unit, evidences the presence of a similar trend on changing the metal ion, but the electronic interactions are unexpectedly smaller. This decreased electronic interaction could be a consequence of the achievement of an unfavourable conformation. One would expect, on the mere basis of the reduced steric hindrance featured by the OAP unit, an increased electronic interaction as a consequence of the closer contact between the porphyrinic frameworks. This favourable effect, however, may be negatively counterbalanced by the increased charge distribution on the OAP unit, which, in a face-to-face geometry, would result in the onset of repulsive forces. The system would then be forced to assume a more slipped, offset orientation.[24] Further studies, however, are needed in order to shed more light on this point.

Table 3 Luminescence properties[a] of the investigated diporphyrin receptors and their metal ion complexes[b]

	1a			1b			1c			2		
Cation	λ_{max}	Φ	τ	λ_{max}	Φ	τ	λ_{max}	Φ	τ	λ_{max}	Φ	τ
None	652	1.0	8.2	652	1.0	8.2	652	1.0	8.3	652	1.0	9.2
Na^+	650	0.9	8.7	652	1.0	8.6	651	0.9	8.4	652	1.0	8.8
K^+	650	1.0	8.4	653	1.0	8.4	652	0.9	8.5	652	1.0	9.0
Mg^{2+}	651	0.9	7.8	653	1.0	8.1	651	1.0	8.2	652	1.0	8.9
Ca^{2+}	651	0.9	8.0	652	1.0	8.4	651	0.9	8.4	652	0.9	8.7
Sr^{2+}	650	0.9	8.0	651	0.9	8.8	650	0.9	8.3	652	0.9	9.1
Ba^{2+}	650	0.9	8.5	652	0.9	8.9	652	0.9	8.3	652	0.9	9.3

[a] λ_{max} in nm, τ in ns. [b] Porphyrin concentration: 1×10^{-6} M, (MeCN–$CHCl_3$ 1 : 1, v/v), 298 K.

fluorescence quantum yield of free base porphyrins, this could allow one to monitor complexation even when the absorbance due to the dimer is very low (<0.01), and changes can not be observed by means of the less sensitive spectrophotometric technique. Of course, in order to obtain efficient chemosensors higher association constants and more efficient signal transduction mechanisms should be achieved. In this context, the case of the unsymmetric diad is very interesting. Unfortunately in our system the energy transfer mechanism was so effective even in the absence of metal ions that the approach of the two porphyrin units caused by complexation does not induce any further change in the fluorescence spectrum. This indicates that, in order to have an effective switching off/on of the energy transfer mechanism, in the free species the distance between the two chromophores, according to eqn. 2, should be higher than 26 Å and we are actually working in this direction.

Conclusions and future perspectives

Diporphyrin derivatives constitute attractive models of the key enzymatic apparatus involved in life sustaining cycles. The systems we investigated possess the promising feature of a tunable geometry by interaction with a series of alkali and alkaline-earth metal ions. The promoted conformational variations are substantially dependent on the ionic radii of the interacting metal ions and on the lengths of the spacers. This strategy may indeed represent a relevant step toward the design and realisation of systems possessing a promising versatility, arising from the possibility of tuning the geometry, the flexibility and, consequently, the affinity of the resulting receptor for substrate recognition[26] and catalysis.[27]

In addition, it is worth underlining that the complexation process induces noticeable changes in photophysical processes, leading to the possibility to monitor the association event between **1a**–**1c** and **2** and metal cations even at low concentrations. Although a desirable on–off behaviour has not been achieved with these systems, the results obtained are a good starting point for the design of efficient chemosensors.

Experimental

Instrumentation

^{1}H NMR spectra were recorded with a Bruker AC 300 P (300 MHz) spectrometer equipped with a sample tube thermostation apparatus. Chemical shifts are given in ppm relative to tetramethylsilane (TMS) and are referenced against residual solvent signals. Numbering of carbon atoms follows the labelling scheme. Routine UV-visible spectra were measured on a Varian Cary 1E spectrophotometer, whereas more delicate measurements were performed on a Perkin-Elmer λ40 spectrophotometer equipped with a thermostatted cell holder. Uncorrected emission and corrected excitation spectra were obtained with a Perkin-Elmer LS 50 spectrofluorimeter. The fluorescence lifetimes (uncertainty ± 5%) were obtained with an Edinburgh single-photon counting apparatus, in which the flash lamp was filled with D_2. Luminescence quantum yields (uncertainty ± 15%) were determined using H_2TPP in toluene ($\phi = 0.11$) as a reference. In order to allow comparison among emission intensities, we performed corrections for instrumental response, inner filter effects, and phototube sensitivity. A correction for differences in the refraction index was introduced when necessary. Mass spectra (FAB) were recorded on a VG Quattro spectrometer by using *m*-nitrobenzyl alcohol (NBA, Aldrich) as a matrix in the positive ion mode.

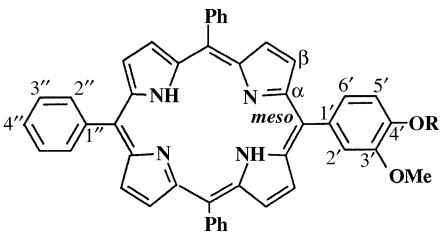

Materials

Silica gel 60 (70–230 mesh) was used for column chromatography. Reagents (Aldrich, Merck or Fluka) were of the highest grade available and were used without further purification. Metal salts employed in the NMR titrations were of the highest anhydrous grade available (Aldrich, Fluka), vacuum dried and stored under a dry atmosphere. The α,ω-ditosylates were prepared according to published procedures.[28] Solvents were dried, distilled and degassed prior to use, by using standard procedures.[29] A small amount of activated 4 Å molecular sieves was added to NMR solvents in order to remove traces of water. Solvents used for the spectrophotometric measurements, acetonitrile and chloroform (Uvasol, Merck), were stored over activated molecular sieves.

^{1}H NMR titration

A $CDCl_3$–CD_3CN 1 : 1 v/v solvent mixture was used for solubility reasons. The temperature was held constant, within ±0.2 K, at 298 K. A general procedure for the ^{1}H NMR titrations is as follows. Solutions of metal ions (1×10^{-3}–5×10^{-2} M) were prepared by dissolving in a 2 mL volumetric flask the required amount of salt in a solution of diporphyrin receptor. The resulting solution was added portionwise *via* a microsyringe to 500 μL of the porphyrin solution (typically 5×10^{-4} M) placed in a thermostatted NMR sample tube. This procedure ensures a constant concentration of the receptor throughout the NMR titration.

Data analysis

The stability constants (K) for 1 : 1 complexation were calculated from the chemical shifts of chosen signals. The values obtained for different sets of signals were the same within experimental error (≤5%). The equation used for analysing NMR titration data was of the general form:[30]

$$\Delta\delta_{obs} = \Delta\delta_i K[M^{n+}]/(1 + K[M^{n+}]) \quad (3)$$

where $\Delta\delta_{obs} = \delta_{obs} - \delta_0$, δ_{obs} is the observed NMR shift of a specific acceptor proton in the equilibrium solution, δ_0 the shift of the free acceptor proton, $\Delta\delta_i = \delta_i - \delta_0$, δ_i is the shift of the concerned proton of the M^{n+}–receptor complex, and $[M^{n+}]$ is the total concentration of the added salt. The unknown parameters, $\Delta\delta_i$ and K, were obtained by the least-squares curve fitting program Kaleidagraph©[31] from six to eight measurements. In the case of Ba^{2+} and Sr^{2+}, characterised by higher binding constants, an excess of salt was not possible and eqn. 4 was necessarily used[32]

$$K = (\Delta\delta_{obs}/\Delta\delta_i)/([M^{2+}][1 - (\Delta\delta_{obs}/\Delta\delta_i)]) \quad (4)$$

where $[M^{2+}] = [M^{2+}]_t - (\Delta\delta_{obs}/\Delta\delta_i)[P]_t$; $[M^{2+}]$ is the free metal concentration, $[M^{2+}]_t$ the total concentration of the added metal cation, and $[P]_t$ the total concentration of the porphyrinic host. The regression values (r^2) for the computer fitting were better than 0.996. Experiments were run in duplicate and found to be in excellent agreement within experimental error (standard deviation ≤5%).

Preparations

5-(4-Hydroxy-3-methoxyphenyl)-10,15,20-triphenylporphyrin, 3a. To a solution of 8.2 g (77 mmol) of benzaldehyde and 1.0 g (7.8 mmol) of 4-hydroxy-3-methoxybenzaldehyde (vanillin) in 400 mL of refluxing acetic acid, a solution of 5.5 g (83 mmol) of pyrrole in 50 mL of acetic acid

was added dropwise over a period of 30 min. The reaction mixture was stirred at reflux temperature for 3 h, then cooled to room temperature and left overnight. The crystalline residue, separated from the bulk of the reaction mixture by filtration, was washed repeatedly with methanol. 1.5 g of shiny dark purple crystals, consisting of a mixture of two products, was chromatographed on SiO_2. Elution with a hexane–30% chloroform mixture gave an initial moving band containing the *meso*-H_2TPP co-product. The desired porphyrin was subsequently eluted with a 1% methanol–chloroform mixture to give 0.6 g (0.9 mmol, 12% yield) of **3a** as a purple crystalline solid. The product was used in subsequent Williamson coupling reactions without further purification. ^{1}H NMR ($CDCl_3$): δ 8.9–8.8 (m, 8H, β-H), 8.3–8.2 (m, 5H, C_6H_5), 7.8–7.7 (m, 12H, C_6H_5 + aromatics), 7.31 (d, $J = 8.1$ Hz, 1H, aromatics), 5.97 (brs, 1H, OH), 4.0 (s, 3H, OMe) and −2.76 (brs, 2H, NH). ^{13}C NMR ($CDCl_3$): δ 151.2 (C-α), 145.6 (C-3′), 144.9 (C-4′), 142.2 (C-1″, C_6H_5), 134.6 (C-1′), 134.2 (C-2″), 131.0 (C-β), 127.7 (C-4″), 126.7 (C-3″), 120.1 (C-*meso*), 120.0 (C-*meso*), 117.6 (C-5′), 117.6 (C-2′) and 56.2 (OMe). UV-vis ($CDCl_3$): λ_{max}/nm (log ε) 420 (5.48, Soret), 517 (4.13), 552 (3.82), 590 (3.64) and 648 (3.62). FAB-MS (NBA): m/z 660, $[M]^+$.

1,8-Bis[2-methoxy-4-(10,15,20-triphenyl-5-porphyrinyl)-phenoxy]-3,6-dioxaoctane, 1a. 100 mg of porphyrin **3a** (0.152 mmol), 34 mg of triethylene glycol ditosylate (0.075 mmol) and an excess of anhydrous K_2CO_3 (250 mg) in 10 mL of freshly dried and distilled DMF were stirred at reflux temperature overnight under argon. The mixture was then filtered and the solvent stripped off *in vacuo* to give a purple residue which was dissolved in chloroform (50 mL) and washed with brine (3 × 100 mL) and then water until neutral. The organic solution was dried (Na_2SO_4), reduced to a small volume and chromatographed (SiO_2) eluting with a 3% methanol–chloroform solvent mixture to give 180 mg (0.122 mmol, 82% yield) of the desired diporphyrin product. ^{1}H NMR ($CDCl_3$): δ 8.9–8.8 (m, 8H, β-H pyrrolic), 8.2–8.1 (m, 5H, C_6H_5), 7.8–7.7 (m, 11H, C_6H_5 + aromatics), 4.6–4.5 (brt, $J = 3.6$, 2H, ArOCH_2CH_2O), 4.2–4.1 (brt, $J = 3.6$ Hz, 2H, ArOCH$_2$CH_2O), 4.0 (s, 2H, OCH$_2$CH$_2$O), 3.9 (s, 3H, ArOCH$_3$) and −2.7 (brs, 2H, NH). ^{13}C NMR ($CDCl_3$): δ 148.2 (C-3′), 147.6 (C-4′), 142.1 (C-1″, C_6H_5), 135.3 (C-1′) 135.5 (C-2″, C_6H_5), 131.1 (C-α), 127.7 (C-β), 127.4 (C-4″, C_6H_5), 126.9 (C-3″, C_6H_5), 120.1 (C-*meso*), 120.0 (C-*meso*), 119.9 (C-*meso*), 118.8 (C-5′), 111.6 (C-2′), 71.1 (ArOCH$_2$CH$_2$O), 70.0 (ArOCH$_2$CH$_2$O), 68.7 (OCH$_2$CH$_2$O) and 56.1 (OMe). UV-vis ($CHCl_3$): λ_{max}/nm (log ε) 419 (6.16, Soret), 516 (4.76), 551 (4.46), 590 (4.31) and 646 (4.12) FAB-MS (NBA): cluster centred at m/z 1430, $[M]^+$.

1,11-Bis[2-methoxy-4-(10,15,20-triphenyl-5-porphyrinyl)-phenoxy]-3,6,9-trioxaundecane, 1b. The procedure employed for the preparation of compound **1a** was followed. Starting from 100 mg (0.15 mmol) of porphyrin **3a**, and 39 mg of tetraethylene glycol ditosylate (0.075 mmol), 180 mg of porphyrin **1b** (0.12 mmol, 80% yield) were obtained. ^{1}H NMR ($CDCl_3$): δ 8.9–8.8 (m, 8H, β-H pyrrolic), 8.2–8.1 (m, 5H, aromatics), 7.7–7.6 (m, 11H, C_6H_5 + aromatics), 4.47 (brt, $J = 5.4$ Hz, 2H, OCH_2CH$_2$O), 4.10 (m, 2H, OCH$_2$CH_2O), 3.95 (s, 3H, CH$_3$O), 3.9–3.8 (m, 4H, OCH$_2$CH$_2$O), and −1.49 (brs, 2H, NH). ^{13}C NMR ($CDCl_3$): δ 148.2 (C-3′), 147.6 (C-4′), 142.1 (C-1″, C_6H_5), 135.2 (C-1′), 134.5 (C-2″, C_6H_5), 131.0 (C-α), 127.7 (C-β), 127.4 (C-4″, C_6H_5), 126.7 (C-3″, C_6H_5), 120.1 (C-*meso*), 119.9 (C-6′), 118.8 (C-5′), 111.6 (C-2′), 71.0 (ArOCH$_2$CH$_2$O), 70.8 (ArOCH$_2$CH$_2$O), 69.9 (OCH$_2$CH$_2$O), 68.7 (OCH$_2$CH$_2$O) and 56.1 (CH$_3$O). UV-vis ($CHCl_3$): λ_{max}/nm (log ε) 419 (6.12, Soret), 516 (4.78), 551 (4.43), 590 (4.30) and 646 (4.13). FAB-MS (NBA): cluster centred at m/z 1478, $[M]^+$.

1,14-Bis[2-methoxy-4-(10,15,20-triphenyl-5-porphyrinyl)-phenoxy]-3,6,9,12-tetraoxatetradecane, 1c. The procedure employed for the preparation of compound **1a** was followed. Starting from 120 mg (0.182 mmol) of porphyrin **3a** and 36.2 mg (0.0721 mmol) of pentaethylene glycol ditosylate, 215 mg (0.145 mmol, 80% yield) of porphyrin **2c** were obtained. ^{1}H NMR ($CDCl_3$): δ 8.9–8.8 (m, 8H, β-H), 8.2–8.1 (m, 5H, C_6H_5), 7.7–7.6 (m, 12 H, C_6H_5), 4.47 (brt, $J = 5.4$ Hz, 2H, ArOCH_2CH$_2$O), 4.1 (m, ArOCH$_2$CH_2O), 3.95 (s, 3H, OCH$_3$), 3.9–3.8 (m, 4H, OCH$_2$CH$_2$O) and −1.49 (brs, 2H, NH). ^{13}C NMR ($CDCl_3$): δ 148.2 (C-3′), 147.6 (C-4′), 142.1 (C-1″, C_6H_5), 135.2 (C-1′), 134.5 (C-2″, C_6H_5), 131.0 (C-α), 127.7 (C-β), 127.4 (C-4″, C_6H_5), 126.7 (C-3″, C_6H_5), 120.1 (C-*meso*), 119.9 (C-6′), 118.8 (C-5′), 111.6 (C-2′), 71.0 (ArOCH_2CH$_2$O), 70.8 (ArOCH$_2$CH_2O), 69.9 (OCH$_2$CH$_2$O), 68.7 (OCH$_2$CH$_2$O) and 56.1 (OCH$_3$). UV-vis ($CHCl_3$): λ_{max}/nm (log ε) 419 (6.16, Soret), 516 (4.78), 551 (4.46), 590 (4.28) and 646 (4.13). FAB-MS (NBA): cluster centred at m/z 1510, $[M - H]^+$.

2-[2-(2-(2-(10,15,20-triphenyl-5-porphyrinyl)-1-oxo-2-methoxyphenyl)ethoxy)ethoxy)ethoxy]ethanol, 3b. 100 mg of porphyrin precursor **3a** (0.152 mmol), 58 mg of tetraethylene glycol monotosylate (0.167 mmol) and an excess of anhydrous K_2CO_3 (250 mg) in 10 mL of freshly dried and distilled DMF were stirred at reflux temperature overnight under argon. The mixture was then filtered and the solvent stripped off *in vacuo* to give a purple residue which was dissolved in chloroform (50 mL) and washed with brine (3 × 100 mL) and then water until neutral. The organic solution was dried (Na_2SO_4), reduced to a small volume and chromatographed (SiO_2) eluting with a 3% methanol–chloroform solvent mixture to give a purple solid residue which was further crystallised ($CHCl_3$–hexane) to give 114 mg (0.136 mmol, 90% yield) of the desired product. ^{1}H NMR ($CDCl_3$): δ 8.9–8.8 (m, 8H, β-H), 8.2 (m, 5H), 7.5 (m, 2H), 4.4–3.6 (m, 16H, OCH$_2$CH$_2$O), 3.96 (s, 3H, OCH$_3$), 2.21 (brs, 1H, OH) and −2.75 (brs, 2H, NH). UV-vis ($CHCl_3$): λ_{max} 419 (Soret), 516, 551, 590 and 647 nm. FAB-MS (NBA): m/z 837 (35, $[M]^+$) and 876 (100%, $[M + K]^+$).

1-[2-Methoxy-4-(10,15,20-triphenyl-5-porphyrinyl)-phenyoxy]-11-(*p*-tolylsulfonyloxy)-3,6,9-trioxaundecane, 3c. 114 mg of porphyrin **3b** and 130 mg of *p*-toluenesulfonyl chloride (61 mmol) were dissolved in 25 mL of dry pyridine. The reaction mixture was stirred for 12 h under an argon atmosphere, then diluted with chloroform (250 mL) and washed with aqueous hydrochloric acid (3%), then with water until neutral. The organic phase was dried (Na_2SO_4) and evaporated under reduced pressure to give 110 mg of compound **3c** (0.10 mmol, 80% yield) which was used without further purification in the subsequent coupling reaction. ^{1}H NMR ($CDCl_3$): δ 8.9–8.8 (m, 8H, β-H pyrrolic), 8.3–3.2 (m, 5H, C_6H_5), 7.8–7.7 (m, 14H, C_6H_5 + aromatics), 7.31 (d, $J = 8.1$, 1H, aromatics), 7.30 (d, $J = 9.1$ Hz, 2H, 3′-Ts), 5.97 (brs, 1H, OH), 4.2–3.6 (m, 16H, OCH$_2$CH$_2$O), 4.0 (s, 3H, OMe), 2.13 (s, 3H, Ar CH_3) and −2.77 (brs, 2H, NH). UV-vis ($CHCl_3$): λ_{max} 419 (Soret), 516, 551, 590 and 670 nm. FAB-MS (NBA): m/z 990 $[M]^+$.

13,17-Diethyl-2,3,7,8,12,18-5-(4-hydroxy-3-methoxyphenyl)-hexamethylporphyrin, 4. 0.5 g of 8,12-diethyl-2,3,7,13,17,18-hexamethylbiladiene-*a*,*c* dibromide[10] (0.87 mmol), 4-hydroxy-3-methoxybenzaldehyde (0.12 g, 0.87 mmol), and *p*-toluene sulfonic acid (1 g) were dissolved in 250 mL of ethanol. The reaction mixture was refluxed for 4 h. An excess of sodium acetate (1.5 g) was added in order to neutralise the solution. The mixture was then evaporated under reduced pressure and the solid dark residue dissolved in the minimum amount of

dichloromethane and chromatographed on neutral alumina (Grade III) eluting with CH_2Cl_2. A red–violet band was collected and evaporated to afford 350 mg (0.6 mmol, 72% yield) of compound **4** which was used in the subsequent coupling reaction without further purification. ^{1}H NMR ($CDCl_3$): δ 10.15 (s, 2H, *meso*-H), 9.94 (s, 1H, *meso*-H), 7.6–7.3 (m, 3H, aromatics), 5.99 (s, 1H, OH), 4.07 (q, $J = 7.56$, 2H, CH_2CH_3), 3.95 (s, 3H, OCH_3), 3.63 (s, 3H, CH_3), 2.56 (s, 3H, CH_3), 1.86 (t, $J = 7.56$ Hz, 3H, CH_2CH_3) and −3.22 (brs, 1H, NH). ^{13}C NMR ($CDCl_3$): δ 146.1 (C-3′), 146.0 (C-4′), 145.4 (C-α), 143.8 (C-α), 142.8 (C-α), 141.7 (C-α), 137.8 (C-β), 137.0 (C-β), 135.6 (C-β), 134.7 (C-1′, C_6H_4OR), 118.5 (C-6′, C_6H_4OR), 116.1 (C-5′, C_6H_4OR), 113.7 (C-2′, C_6H_4OR), 96.6 (C-*meso*), 95.3 (C-*meso*), 56.3 (OCH_3), 19.8 (CH_2), 17.6 (CH_3), 14.9 (CH_3), 12.2 (CH_3) and 11.6 (CH_3). UV-vis ($CHCl_3$): λ_{max}/nm 404 (Soret), 502, 536, 571 and 623. FAB-MS (NBA): m/z 572 [M^+].

1-[2,4-(13,17-Diethyl-2,3,7,8,12,18-hexamethyl-5-porphyrinyl)-2-methoxyphenoxy]-11-[2-methoxy-4-(10,15,20-triphenyl-5-porphyrinyl)phenoxy]-3,6,9-trioxaundecane, 2. 110 mg of porphyrin derivative **3c** (0.11 mmol), 77 mg of **4** (0.13 mmol) and an excess of anhydrous K_2CO_3 (250 mg) in 25 mL of freshly dried and distilled DMF were stirred at 80 °C overnight under argon. The mixture was then filtered and the solvent stripped off *in vacuo* to give a purple residue which was dissolved in chloroform (50 mL) and washed with brine (3 × 100 mL) and then water until neutral. The organic solution was dried (Na_2SO_4), reduced to a small volume and chromatographed (SiO_2) eluting with a 3% methanol–chloroform solvent mixture. The appropriate fraction was collected and evaporated under reduced pressure to give a purple-red solid residue which was crystallised (chloroform–hexane) to give 31 mg (0.02 mmol, 20% yield) of the desired diporphyrin product as a purple crystalline solid. ^{1}H NMR ($CDCl_3$): δ 10.2–9.9 (m, 3H, *meso*-H), 8.9–8.8 (m, 8H, β-H), 8.2–8.1 (m, 5H, aromatics), 7.8–7.5 (m, 12H, aromatics), 6.89 (d, $J = 2.3$ Hz, 1H, 3′-H), 4.5–4.4 (brt, $J = 5.0$ Hz, 2H, $ArOCH_2CH_2O$), 4.2–3.6 (m, 13H, $OCH_2CH_2O + OCH_3 + \beta$-$CH_2CH_3$), 3.5 (s, 3H, β-$CH_3$), 2.50 (s, 3H, β-$CH_3$), 1.9–1.8 (m, 3H, β-$CH_2CH_3$) and −2.8 (brs, 2H, NH). UV-vis ($CHCl_3$): λ_{max}/nm (log ε) 407 (5.97, Soret), 419 (6.03, Soret), 511 (4.86), 536 (4.73), 550 (4.50), 586 (4.26), 624 (4.10), 647 (4.13) and 675 (3.89). FAB-MS (NBA): m/z 1390 [M]$^+$.

Acknowledgements

We are indebted to Mr Alessandro Leoni for his valuable technical help. We also thank Professor Gianfranco Ercolani, University of "Tor Vergata", for helpful discussions. CNR (STM programme 1998) and MURST (Project no. 98032774402) are gratefully acknowledged for funding.

References and notes

1 (*a*) M. R. Wasielewski, *Chem. Rev.*, 1992, **92**, 435; (*b*) H. Kurreck and M. Huber, *Angew. Chem., Int. Ed. Engl.*, 1995, **34**, 849; (*c*) M. D. Ward, *Chem. Soc. Rev.*, 1997, **26**, 365; (*d*) G. Hungerford, M. Van der Auweraer, J.-C. Chambron, V. Heitz, J.-P. Sauvage, J.-L. Pierre and D. Zurita, *Chem. Eur. J.*, 1999, **5**, 2089; (*e*) K. M. Kadish, N. Guo, E. Van Caemelbeche, A. Froiio, R. Paolesse, D. Monti, P. Tagliatesta, T. Boschi, L. Prodi, F. Bolletta and N. Zaccheroni, *Inorg. Chem.*, 1998, **37**, 2358; (*f*) S. Tsuchiya, *J. Am. Chem. Soc.*, 1999, **121**, 48; (*g*) C. Ikeda, N. Nagahara, E. Motegi, N. Yoshioka and H. Inoue, *Chem. Commun.*, 1999, 1759; (*h*) C. C. Mak, N. Bampos and J. K. M. Sanders, *Chem. Commun.*, 1999, 1085; (*i*) A. Okomura, K. Funatsu, Y. Sasaki and T. Imamura, *Chem. Lett.*, 1999, 779; (*j*) N. Nagata, S.-i. Kugimiya and Y. Kobuke, *Chem. Commun.*, 2000, 1389; (*k*) For a recent overview on non-covalent multiporphyrin assemblies see: J.-C. Chambron, V. Heitz and J.-P. Sauvage, in *The Porphyrin Handbook*, ed. K. M. Kadish, K. M. Smith and R. Guilard, Academic Press, London, 2000, vol. 6, ch. 40, p. 1.

2 J. Deisenhofer and H. Michel, *Science*, 1989, **245**, 1463.

3 (*a*) J. P. Collman, P. S. Wagenknecht and J. E. Hutchinson, *Angew. Chem., Int. Ed. Engl.*, 1994, **33**, 1537, and references therein; (*b*) J. P. Collman, *Inorg. Chem.*, 1997, **36**, 5145; (*c*) Y. Deng, C. J. Chang and D. G. Nocera, *J. Am. Chem. Soc.*, 2000, **122**, 410, and references therein; (*d*) The synthesis of a "face-to-face" porphyrin–corrole, as a potential catalyst for four-electron reduction of dioxygen, has recently been reported: F. Jerome, C. P. Gros, C. Tardieu, J.-M. Barbe and R. Guilard, *New J. Chem.*, 1998, **22**, 1327. For an overview of the role of porphyrins as synthetic models of hemoglobin and myoglobin see: (*e*) J. P. Collman and L. Fu, *Acc. Chem. Res.*, 1999, **32**, 455; (*f*) T. Ayashi and H. Ogoshi, *Chem. Soc. Rev.*, 1997, **26**, 355; (*g*) M. Momenteau and C. A. Reed, *Chem. Rev.*, 1994, **94**, 659.

4 H. B. Dunford, *Heme Peroxidases*, Wiley-WCH Editions, New York, 1999; P. R. Ortiz de Montellano, *Cytochrome P-450: Structure, Mechanisms and Biochemistry*, 2nd edn., Plenum, New York, 1995; M. Wikström, K. Krab and M. Saraste, *Cytochrome Oxidase: A Synthesis*, Academic Press, London, 1981; B. K. Burgess, *Chem. Rev.*, 1990, **90**, 1377.

5 D. Monti, M. Venanzi, G. Mancini, F. Marotti, L. La Monica and T. Boschi, *Eur. J. Org. Chem.*, 1999, 1901.

6 For a critical approach to the topic, see: M. G. H. Vicente, L. Jaquinod and K. M. Smith, *Chem. Commun.*, 1999, 1771.

7 A. P. de Silva, H. Q. N. Gunaratne, T. Gunnlaughsson, A. J. M. Huxley, C. P. McCoy, J. T. Rademacher and T. E. Rice, *Chem. Rev.*, 1997, **97**, 1515; L. Fabbrizzi, M. Licchelli, P. Pallavicini, L. Parodi and A. Taglietti, *Transition Metals in Supramolecular Chemistry, Perspectives in Supramolecular Chemistry*, ed. J. P. Sauvage, John Wiley and Sons, Chichester, 1999, vol. 5, ch. 3, pp. 93–134.

8 I. Tabushi, S. Kugimiya, M. G. Kinnaird and T. Sasaki, *J. Am. Chem. Soc.*, 1985, **107**, 4192.

9 H. Feuer and J. Hooz, *The Chemistry of the Ether Linkage*, Interscience Publishers, New York, 1967, ch. 10.

10 J. S. Lindsey, I. C. Schreiman, H. C. Su, P. C. Kearney and M. Marguerettas, *J. Org. Chem.*, 1987, **52**, 827.

11 K. Kalyanasundaram, *Photochemistry of Polypyridine and Porphyrin Complexes*, Academic Press, London, 1991.

12 (*a*) T. H. Föster, *Discuss. Faraday Soc.*, 1959, **27**, 7; (*b*) D. L. H. Dexter, *Chem. Phys.*, 1953, **21**, 836.

13 A. Osuka, K. Maruyama, I. Yamazaki and N. Tamai, *Chem. Phys. Lett.*, 1990, **165**, 392; J. L. Sessler, B. Wang and A. Harriman, *J. Am. Chem. Soc.*, 1995, **117**, 704.

14 N. C. Fletcher, M. D. Ward, S. Encinas, N. Armaroli, L. Flamigni and F. Barigelletti, *Chem. Commun.*, 1999, 2089.

15 D. Live and S. Chang, *J. Am. Chem. Soc.*, 1976, **98**, 3769. The cation–receptor electrostatic interactions are evidenced by chemical shift variation of the oxaethylenic segments that closely parallel the charge density of the cation ($Li^+ \approx Na^+ > K^+ > Cs^+$).

16 The cation-labelling procedure is a powerful means for characterisation of supramolecular structures and aggregates by FAB, MALDI-TOF, and ESI mass spectroscopy: M. Lämsä, J. Huuskonen, K. Rissanen and J. Pursianen, *Chem. Eur. J.*, 1998, **4**, 84; P. Timmerman, K. A. Jolliffe, M. C. Crego Calama, J.-L. Weidmann, L. J. Prins, F. Cardullo, B. H. M. Snelling-Ruël, R. H. Fokkens, N. M. M. Nibbering, S. Shinkai and D. N. Reinhoudt, *Chem. Eur. J.*, 2000, **6**, 4104; C. A. Schalley, J. M. Riveira, T. Martín, J. Santamaría, G. Siuzdak and J. Rebeck, Jr, *Eur. J. Org. Chem.*, 1999, 1325.

17 Compare for example the association constant of compound **1b** to that of the earlier reported tetraspacered counterpart (ref. 5). This effect, known as "donor end group effect", is usually encountered in the case of related podands bearing aromatic ends, and is accounted for by a favourable enthalpic contribution exerted by the additional binding sites: B. Tümmler, G. Maas, F. Fögtle, H. Sieger, U. Heimann and E. Weber, *J. Am. Chem. Soc.*, 1979, **101**, 2588; B. Tümmler, G. Maass, E. Weber, W. Wehner and F. Fögtle, *J. Am. Chem. Soc.*, 1977, **99**, 4683.

18 (*a*) T. R. Jonson and J. J. Katz, in *The Porphyrins*, ed. D. Dolphin, Academic Press, New York, 1978, vol. 4, ch. 1, pp. 1–59. For a recent paper on the structure determination of supramolecular architectures, by complexation-induced ^{1}H NMR chemical shift changes, see for example: (*b*) C. A. Hunter and M. J. Packer, *Chem. Eur. J.*, 1999, **5**, 1891.

19 The increased ring current effect, caused by the presence of the electron donating alkyl groups, results in a pronounced upfield shift of the inner N–H pyrrolic resonances (see Experimental section). For additional examples see ref. 18(*a*).

20 R. D. Shannon, *Acta Crystallogr., Sect. A*, 1976, **32**, 751.
21 R. M. Izatt, K. Pawlak and J. S. Bradshaw, *Chem. Rev.*, 1995, **95**, 2529; F. C. J. M. van Veggel, W. Verboom and D. N. Reinhoudt, *Chem. Rev.*, 1994, **94**, 279; R. M. Izatt, K. Pawlak, J. S. Bradshaw and R. L. Brueing, *Chem. Rev.*, 1991, **91**, 1721; F. Vögtle and E. Weber, in *Crown Ethers and Analogs*, ed. S. Patai and Z. Rappoport, John Wiley and Sons, New York, 1989, ch. 4, pp. 207–304; R. M. Izatt, J. S. Bradshaw, S. A. Nielsen, J. D. Lamb and J. J. Christensen, *Chem. Rev.*, 1985, **85**, 271. Nice evidence for the high affinity shown by Sr^{2+} and Ba^{2+} for **1b** is given by the broadening of the NMR signal upon the first additions of metal salts to the porphyrin solution (ESI Fig. S2).† This effect can be ascribed to the presence of both the free and the metal-bound receptor in slow exchange on the NMR timescale. At a concentration of the added metal ion close to the equivalence point, *i.e.* in the range where the bound species predominates, narrowing of the signals occurs. It has been reported that, in the case of related acyclic systems [see for example ref. 18(*b*)], the decomplexation rate constants (k_{out}) are generally several orders of magnitude smaller than the formation rate constants (k_{in}). In our case a rough estimate of the decomplexation rate constant $k_{out} \approx 10^3$–10^4 s^{-1} is consistent with reported values.
22 R. Tahara, T. Morozumi, Y. Suzuki, Y. Kakizawa, T. Akita and H. Nakamura, *J. Incl. Phenom. Mol. Recognit. Chem.*, 1998, **32**, 283; J. Kawakami, Y. Komai and S. Ito, *Chem. Lett.*, 1996, 617; Y. Kakizawa, T. Akita and H. Nakamura, *Chem. Lett.*, 1993, 1671; Y. Kobuke and H. Watanabe, *J. Incl. Phenom. Mol. Recognit. Chem.*, 1998, **32**, 347; it has been reported that some "metal-organised crowns" show noticeable selectivity for alkali metal ions over alkaline earth analogues: Y. Kobuke, K. Kokubo and M. Munakata, *J. Am. Chem. Soc.*, 1995, **117**, 12751.
23 The absence of a splitting of the Soret band by exciton coupling of the macrocycles rules out the occurrence of an edge-to-edge type conformation: J. H. Fuhrhop and J. Köning, in *Membranes and Molecular Assemblies: The Synkinetic Approach*, Monographs in Supramolecular Chemistry, ed. J. F. Stoddart, The Royal Society of Chemistry, Cambridge, 1994; K. Kano, H. Minamizono, T. Kitae and S. Negi, *J. Phys. Chem.*, 1997, **101**, 6118; J. H. van Esch, M. C. Feiters, A. M. Peters and R. J. M. Nolte, *J. Phys. Chem*, 1994, **98**, 5541; C. Schell and H. K. Hombrecher, *Chem. Eur. J.*, 1999, **5**, 587.
24 For a discussion on this topic see: C. A. Hunter and J. K. M. Sanders, *J. Am. Chem. Soc.*, 1990, **112**, 5525; C. A. Hunter, *Chem. Soc. Rev.*, 1994, 101.
25 L. Fabbrizzi, M. Licchelli and P. Pallavicini, *Acc. Chem. Res.*, 1999, **32**, 846; L. Fabbrizzi and A. Poggi, *Chem. Soc. Rev.*, 1995, 197; E. Kimura and T. Koike, *Chem. Soc. Rev.*, 1998, **27**, 179.
26 For a recent overview see: H. Ogoshi, T. Mizutani, T. Hayashi and Y. Kuroda, in *The Porphyrin Handbook*, ed. K. M. Kadish, K. M. Smith and R. Guilard, Academic Press, London, 2000, vol. 6, ch. 46, pp. 279–340.
27 Z. Clyde-Watson, A. Vidal-Ferran, L. J. Twyman, C. J. Walter, D. W. J. McCallien, S. Fanni, N. Bampos, R. S. Wylie and J. K. M. Sanders, *New J. Chem.*, 1998, **228**, 493; C. J. Walter, H. L. Anderson and J. K. M. Sanders, *J. Chem. Soc., Chem. Commun.*, 1993, 458; L. G. MacKay, S. Wylie and J. K. M. Sanders, *J. Am. Chem. Soc.*, 1994, **116**, 3141; Y. Murakami, J.-I. Kikuchi, Y. Isaeda and O. Hayashida, *Chem. Rev.*, 1996, **96**, 721; For an interesting discussion on the present role of supramolecular chemistry in catalysis see: J. K. M. Sanders, *Chem. Eur. J.*, 1998, **4**, 1378.
28 M. Ouchi, Y. Inoue, T. Kanzaki and T. Akushi, *J. Org. Chem.*, 1984, **49**, 1408.
29 D. D. Perrin, W. L. F. Armarego and D. E. Perrin, in *Purification of Laboratory Chemicals*, 2nd edn., Pergamon Press, New York, 1980.
30 K. A. Connors, *Binding Constants. The Measurements of Molecular Complex Stability*, John Wiley and Sons, New York, 1987.
31 KaleidaGraph, version 3.0.4 by Abelbeck Software, Synergy Software, Reading, PA 19606, USA.
32 M. K. Amini and M. Shamsipur, *Inorg. Chim. Acta*, 1991, **183**, 65.